Hydrogen-integrated microgrids planning and operation through two-stage stochastic programming with MIP recourse

Jianting Pan Cheng Ma Sirong Dai

May 18, 2024

Nomenclature

Indices and Parameters

t Index of time step

s Index of scenario

h Planck constant

First Stage Variables

A^{PV} The area of PV units (m^2)

$V^{\mathrm{H_2,r}}$ Capacity of hydrogen tank (m^3)

$V^{\mathrm{CO_2,r}}$ Capacity of carbon tank (m^3)

$P^{\mathrm{El,r}}$ Capacity of electrolyzer (kW)

$P^{\mathrm{CH,r}}$ Capacity of $\mathrm{CH_4}$ device (kW)

$P^{\mathrm{C,r}}$ Capacity of carbon tank (kW)

Second Stage Variables

P_t^{PV} Power output of PV units at time t

P_t^{DG} Power output from diesel DG at time t

P_t^{CCS} Power demand from CCS at time t

P_t^{El} Power demand from El at time t

P_t^{C} Power demand from carbon devices at time t

$P_t^{\mathrm{CH_4}}$ Power demand from CH_4 devices at time t

1 Introduction

Microgrids that integrate the on-site renewable energy sources (RES) and hydrogen facilities are promising methods to decarbonize the energy sector [1]. Generally, microgrid is a small-scale self-controlled power system, which regulates and manages a group of interconnected DERs and loads within clearly defined boundaries. Microgrids are often lie in the distribution level and are highly integrated systems [2].

In the context of the "peak carbon and carbon neutrality" objectives, reconciling the escalating energy demand with carbon dioxide emissions has emerged as a shared challenge for the global community [3]. With its long-established reliance on coal for power generation, China faces two key tasks in transitioning to a more modern power system. The first task involves promoting carbon reduction and utilization within existing thermal power units, while the second task encourages the expansion and development of renewable energy consumption [4].

The integration planning of hydrogen-based microgrids needs to be considered under a holistic investment and operational perspective which is shown in Fig. 1.1. Since the high expenses remain as the major challenge to deploy the hydrogen energy facilities on microgrids level. Without a proper resource planning, it will be difficult to recover the investment cost even if the system operations are economically scheduled. Besides, to achieve a higher system performance, the planning outcomes should be sufficiently robust over the multi-type uncertainties of long-run operation, e.g., the intermittent generation of RES devices, the load demand [5].

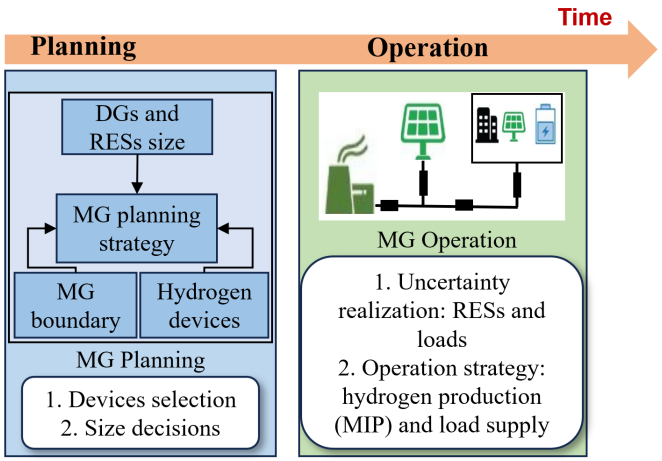

Figure 1.1: The microgrids holistic planning and operation process.

To address these issues, Zhou Xiaoxin et al. [3] introduced the concept of the hydrogen-integrated microgrids. This concept integrates Carbon Capture and Storage (CCS) within thermal power units and Power-to-Gas (P2G) technology, enabling the production of various green fuels during electricity generation. This not only enhances the flexibility of power dispatch but also supports the stable operation of power systems with a high proportion of renewable energy. In addition, it facilitates efficient and environmentally friendly use of carbon capture. The specific description can be viewed in Figure 1.2. The system contains electric loads, renewable energy resources (RESs), DGs, hydrogen devices, and carbon and gas devices.

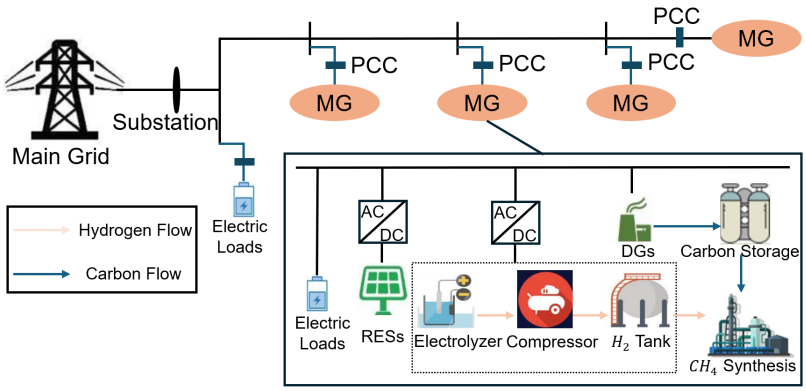

Figure 1.2: Hydrogen-based microgrids with renewable energy sources.

However, the effective implementation and widespread application of hydrogen-integrated microgrids depends on strategic operation scheduling and capacity configuration, which form the foundational support for achieving a synergistic and economically efficient operation of diverse energy sources. Yet, the complex interdependencies between different equipment, the high unpredictability of photovoltaic resources and electricity loads, and the conflicting relationships between

various economic and safety indicators pose significant challenges for the planning and configuration of integrated energy systems.

In the capacity configuration design of microgrids, to make the optimization results as applicable as possible to real-world scenarios, it is essential to fully consider the impact of uncertainties on system optimization. Among these, two-stage stochastic programming, which describes uncertainty through probability distribution, makes the model more aligned with reality and has garnered widespread attention in the field of microgirds [6, 7]. The decision-making framework of a two-stage stochastic programming for optimal energy system operation can be structured in the following way. For instance, in the first stage, the program could involve day-ahead operational commitment decisions for the capacity of the equipment in IEPU. Following this, the second stage could then encompass real-time dispatch decisions. These decisions would need to be made based on the actual realization of uncertain variables such as energy demands and solar patterns. The above research provides a theoretical reference to solve the uncertainty of microgrids through two-stage stochastic programming.

In this report, we aim to develop a two-stage stochastic model for the optimal design of hydrogen-integrated microgrids under conditions of uncertainty. The model will consider all relevant uncertain parameters, including electricity demand and the availability of solar energy. Furthermore, we will employ clustering techniques to characterize this uncertainty accurately. Finally, we would use multi-cut L-shape algorithm to solve this model. To handle the uncertain risks associated with energy sector, our planning problem is formulated as a two-stage stochastic mixed-integer program. The first-stage problem is to optimize the microgrids capacity sizing decisions, including RES devices, electrolyzers, and hydrogen devices. In the second-stage problem, the coordinated electricity-hydrogen scheduling is modeled as an MIP to capture the microgrid's operation under a discrete set of stochastic scenarios. To be more specific, the in-out decisions for hydrogen storage and carbon storage are binary variables since the hydrogen can only be at one of putting in or taking out state at each time step due to the devices limitations.

2 The model of the two-stage stochastic optimization

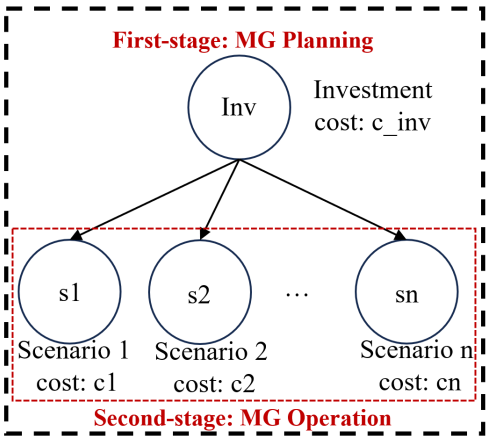

Figure 2.1: Modelling structure for hydrogen-integrated microgrids design under uncertainty using a two-stage stochastic programming model.

The planning and operation model aims to min the total costs, while satisfying the system-level and component-level constraints. First-stage constraints mainly contain devices capacity limitations. Second-stage constraints mainly contains devices operational constraints. Detailed constraints are shown as follows:

2.1 Objective function

$$\min_{x,y} \; C := \sum_{x,y} (C_{inv}(x) + \mathbb{E}(C_{om}(y))), \tag{2.1}$$

where x is the first-stage decision variable and y is the second-stage decision variable.

2.2 Investment constraints

$$0 \leq A^{\mathrm{PV}} \leq A^{\mathrm{PV,r,max}} \tag{2.2a}$$
$$0 \leq V^{\mathrm{H_2,r}} \leq V^{\mathrm{H_2,r,max}} \tag{2.2b}$$
$$0 \leq V^{\mathrm{C,r}} \leq V^{\mathrm{C,r,max}} \tag{2.2c}$$
$$0 \leq P^{\mathrm{El,r}} \leq P^{\mathrm{El,r,max}} \tag{2.2d}$$
$$0 \leq P^{\mathrm{CH,r}} \leq P^{\mathrm{CH,r,max}} \tag{2.2e}$$

where upper and lower bounds for each devices are limited by actual situations.

2.3 Operation constraints

2.3.1 RESs constraints

$$P_t^{\mathrm{PV,r}} = k_t \cdot A^{\mathrm{PV}} \tag{2.3a}$$

$$0 \le P_t^{\mathrm{PV}} \le P_t^{\mathrm{PV,r}} \tag{2.3b}$$

The active power outputs of RESs are mainly determined by the availability of natural resources, as captured by the capacity factors k_t and the maximum dispatchable renewable power source of each time t is $P_t^{\mathrm{PV,r}}$, as shown in Eq. (2.3).

2.3.2 DGs and Carbon devices constraints

$$P^{\mathrm{DG,min}} \le P_t^{\mathrm{DG}} \le P^{\mathrm{DG,max}} \tag{2.4a}$$

$$\Delta P^{\mathrm{DG},-} \le P_t^{\mathrm{DG}} - P_{t-1}^{\mathrm{DG}} \le \Delta P^{\mathrm{DG},+} \tag{2.4b}$$

$$V_t^{\mathrm{CO_2}} = \lambda_1 \cdot P_t^{\mathrm{DG}} \tag{2.5a}$$

$$V_t^{\mathrm{CO_2}} = V_t^{\mathrm{CO_2,in}} + V_t^{\mathrm{cur}} \tag{2.5b}$$

$$P_t^{\mathrm{CCS}} = \lambda_3 \cdot V_t^{\mathrm{CO_2,in}} \tag{2.5c}$$

$$0 \le P_t^{\mathrm{CCS}} \le P^{\mathrm{C,r}} \tag{2.5d}$$

For conventional synchronous-generator-interfaced DGs, the active power output should be bounded as shown in Eq. (2.4). Also, constraints on its ramp-up and ramp-down rates should be satisfied (2.4).

The carbon dioxide emissions of thermal power units are related to output and emission intensity, and the capture amount is determined by the P_t^{DG} and capture efficiency λ_1. The part of capture used to synthesize methane is the actual capture amount, and the dissipation part is V_t^{cur}. CCS power consumption is obtained by multiplying the power consumption coefficient corresponding to unit capture and the actual capture amount, as defined in Eq. (2.5).

2.3.3 Hydrogen devices constraints

$$P_t^{\mathrm{El}} = \lambda_4 \cdot V_t^{\mathrm{H_2,in}} \tag{2.6a}$$
$$0 \le P_t^{\mathrm{El}} \le P^{\mathrm{El,r}} \tag{2.6b}$$
$$P_t^{\mathrm{CH_4}} = \beta \cdot V_t^{\mathrm{CH_4}} \tag{2.6c}$$
$$0 \le P_t^{\mathrm{CH_4}} \le P^{\mathrm{CH_4,r}} \tag{2.6d}$$
$$V_t^{\mathrm{H_2,out}} = \omega_1 \cdot V_t^{\mathrm{CH_4}} \tag{2.6e}$$
$$V_t^{\mathrm{CO_2,out}} = \omega_2 \cdot V_t^{\mathrm{CH_4}} \tag{2.6f}$$

The P2G process synthesizes carbon dioxide captured by CCS and hydrogen produced by electrolyzers into methane. The constraints for this process is shown in Eq. (2.6). The ω_1 and ω_2 are factors for hydrogen and carbon in producing methane. P_t^{El} and $P_t^{\mathrm{CH_4}}$ are power demand from electrolyzers and methane devices at time t.

$$V_t^{\mathrm{H_2}} = V_{t-1}^{\mathrm{H_2}} + V_{t-1}^{\mathrm{H_2,ins}} - V_{t-1}^{\mathrm{H_2,outs}} \tag{2.7a}$$
$$V_{t-1}^{\mathrm{H_2,ins}} = Y_1 \cdot V_{t-1}^{\mathrm{H_2,in}} \tag{2.7b}$$
$$V_{t-1}^{\mathrm{H_2,outs}} = (1 - Y_1) \cdot V_{t-1}^{\mathrm{H_2,out}} \tag{2.7c}$$
$$0 \le V_t^{\mathrm{H_2}} \le V^{\mathrm{H_2,r}} \tag{2.7d}$$
$$V_t^{\mathrm{CO_2}} = V_{t-1}^{\mathrm{CO_2}} + V_{t-1}^{\mathrm{CO_2,ins}} - V_{t-1}^{\mathrm{CO_2,outs}} \tag{2.7e}$$
$$V_{t-1}^{\mathrm{CO_2,ins}} = Y_1 \cdot V_{t-1}^{\mathrm{CO_2,in}} \tag{2.7f}$$
$$V_{t-1}^{\mathrm{CO_2,outs}} = (1 - Y_1) \cdot V_{t-1}^{\mathrm{CO_2,out}} \tag{2.7g}$$
$$0 \le V_t^{\mathrm{CO_2}} \le V^{\mathrm{CO_2,r}} \tag{2.7h}$$

The hydrogen stored in the hydrogen storage equipment at the current moment is related to the hydrogen stored in the equipment at the previous moment and the storage/discharge volume. Therefore, the hydrogen stored in the hydrogen storage device can represent in Eq. (2.7). This constraint is the same for carbon. The Y_1 is the binary variable representing the input/output states of hydrogen and carbon storage devices. The CH_4 product or not is decided also.

2.3.4 Power balance constraints

$$P_t^{\mathrm{PV}} + P_t^{\mathrm{DG}} = P_t^{\mathrm{CH_4}} + P_t^{\mathrm{CCS}} + P_t^{\mathrm{El}} + P_t^{\mathrm{D}} \tag{2.8}$$

The Eq. (2.8) is the the power balance equation for the microgrid. Note that the system's power source is PV and DG, and the main power consumption of the system is electrical loads and hydrogen devices.

2.4 Solution strategy for the two-stage stochastic optimization problem

In this paper, an L-shape method, proposed in [8], is adopted to solve the two-stage stochastic optimization problem. Given this model's constraints and objective function, we now provide the general form of the microgrids design. The first-stage siting and sizing decisions on microgrids are made before revealing the uncertainties. In the second-stage problem, the recourse actions, i.e. the power demand for the devices of microgrids are modeled as an LP under the scenario $s \in S$ with a probability π_s. The full matrix form of the two-state stochastic programming model can be written as:

$$\begin{aligned} &\min_{x,y_s} \; c^\top x + \sum_{s\in S} \pi_s f_s^\top y_s \\ &s.t.\; Ax \geq b,\; Dy_s = B_s x + d_s \quad \forall s \in S \\ &\quad x \geq 0,\; y_s \geq 0, \quad \forall s \in S, \end{aligned} \tag{2.9}$$

where x is the first-stage decision variables and y_s are the second-stage decision variables. Since we can't guarantee all subproblems generating the same type of cuts simultaneously, it will be difficult to combine every subproblems' solutions to generate one single cut. To solve the above model, we introduce the multi-cut L-shape method [9]. We first introduce the following relaxed master problem:

$$\begin{aligned} \underline{z} = \min_{x,\theta_s} \; & c^\top x + \sum_{s\in S} p_s \theta_s \\ \text{s.t. } & Ax \geq b, \quad x \geq 0 \\ & -\left[\pi_{d,s}^{(i)} B_s\right] x \geq \pi_{d,s}^{(i)} d_s \quad i = 1,\ldots,k,\; s \in S \\ & -\left[\pi_s^{(i)} B_s\right] x + \theta_s \geq \pi_s^{(i)} d_s \quad i = 1,\ldots,l,\; s \in S \end{aligned} \tag{2.10}$$

and the subproblem for scenario s is

$$\begin{aligned} (SUB(s)) \quad z_{SUB(s)} = \min_{y_s} \quad & f_s^\top y_s \\ \text{s.t.} \quad & Dy_s = B_s x + d_s \quad : \pi_s \\ & y_s \geq 0. \end{aligned} \tag{2.11}$$

While the subproblem 2.11 might be infeasible for some x that come from solving the relaxed master. This can be determined by solving:

$$\begin{aligned} (SUB - PI(s)) \quad v_{SUB(s)} = \min_{y_s, s^+, s^-} \quad & e^\top s^+ + e^\top s^- \\ \text{s.t.} \quad & Dy_s + s^+ - s^- = B_s x + d_s \quad : \pi_{d,s} \\ & y_s, s^+, s^- \geq 0. \end{aligned} \tag{2.12}$$

The whole algorithm can be summarized as 1.

Algorithm 1 Multi-cut L-shape algorithm

Require: $\bar{z} = +\infty, l = k = 0, \epsilon > 0$.

repeat

(Step 1) Solve the relaxed master problem 2.10. If it is infeasible then stop: the problem is infeasible. Otherwise, let $(\hat{x}, \hat{\theta}_1, ..., \hat{\theta}_S)$ be an optimal solution of 2.10. If no optimality cuts are present, then $\hat{\theta}_1, ..., \hat{\theta}_S$ are deleted from the master and all $\hat{\theta}_1, ..., \hat{\theta}_S = -\infty$. Let $\underline{z} = c^\top \hat{x} + \sum_{s \in S} \pi_s \hat{\theta}_s$.

for $s \in S$ **do**

(Step 2) Solve (SUB-PI(s)) 2.12 with right hand side (RHS) $B_s \hat{x} + d_s$ to obtain $(\hat{v}_{SUB(s)}, \hat{\pi}_{d,s})$. If $\hat{v}_{SUB(s)} > 0$ then append the feasibility cut

$$-\left[\hat{\pi}_{d,s} B_s\right] x \geq \hat{\pi}_{d,s}^{(i)} d_s$$

to the relaxed master problem 2.10 and ignore Step 3 in the current s. Otherwise, go to Step 3.

(Step 3) Solve (SUB(s)) 2.11 to obtain $(\hat{y}_s, \hat{\pi}_s)$. Augment the set of optimality cuts with

$$-\left[\hat{\pi}_s B_s\right] x + \theta_s \geq \hat{\pi}_s d_s$$

to the relaxed master problem 2.10.

end for

(Step 4) Let $\hat{z} = c^\top \hat{x} + \sum_{s \in S} \pi_s f_s^\top \hat{y}_s$. If $\hat{z} < \bar{z}$, then $\hat{z} := \bar{z}$ and $(x^*, y_s^*) := (\hat{x}, \hat{y}_1, ..., \hat{y}_S)$.

until $\bar{z} - \underline{z} \leq \epsilon \min\{|\bar{z}|, |\underline{z}|\}$.

Output: $(x^*, y_1^*, ..., y_S^*)$.

3 Scenario Reduction Analysis

Upon formulating a two-stage SP, the subsequent step involves the construction of probabilistic scenarios, denoted by $s \in S$ for the uncertain parameters. The primary objective of scenario generation in SP is to pinpoint the set of scenarios and their associated probabilities that accurately represent the uncertain parameter space, thereby enabling optimal first- and second-stage decision-making.

However, the utilization of probabilistic scenarios has a significant drawback: it can lead to high computational costs as the problem's size expands with the number of scenarios considered. Therefore, an additional objective is to limit the number of scenarios to a manageable level, ensuring the problem can be resolved with a reasonable computational effort.

By taking historical wind and PV power data of a real-world microgrid, for one year as an example, the scenario set contains 365 curves. The scenario set is reduced to six typical scenarios using the K-means clustering algorithm. The simulation results and original scenario set are shown in Figure 3.3.

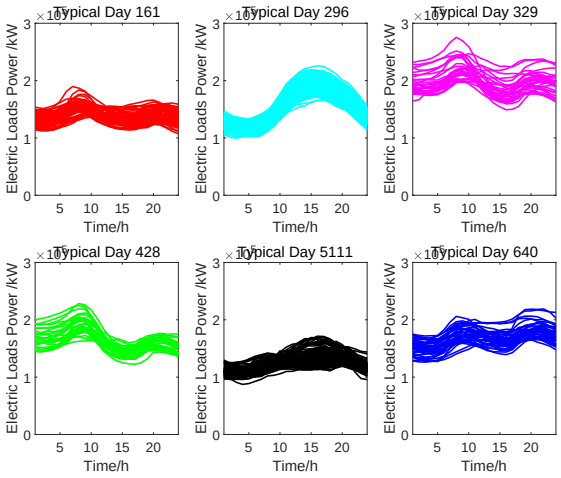

Figure 3.1: Electric load power clustering

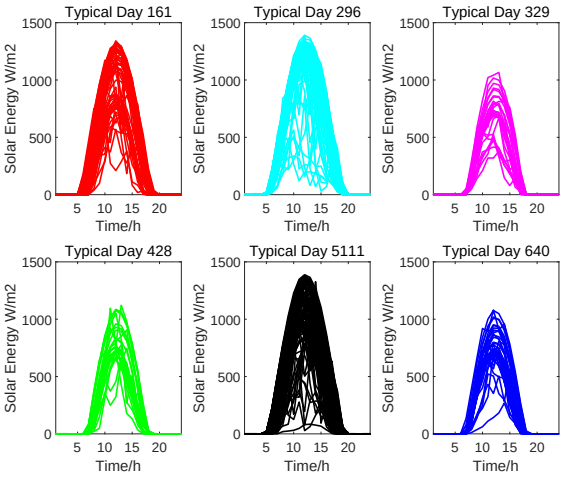

Figure 3.2: Solar energy clustering

Figure 3.3: Scenario clustering

4 Numerical results

In this section, the results of the two-stage stochastic model are presented and analyzed.

We take experiments with MATLAB and GUROBI as the LP solver. Generally, we provide one BENDERS.M function as a multi-cut Benders decomposition solving function with parameters of the matrices and the vectors of the standard problem form as problem (2.9). Since the constraints

of our model is too complicated to transfer to a standard form, we write one specific program PROJECT.M to solve this model with multi-cut Benders decomposition.

4.1 Capacity design

The first-stage decision variables (capacity design) can be seen in Table 4.1.

Equipment	Capacity
PV	152 MW
P2G	100 MW
gas	197 MW
H2 storage	2000 $N.m^3$
CO2 storage	2000 $N.m^3$
The total cost	1.3365×10^7 yuan

Table 4.1: Capacity design

4.2 Electric power balance

The electric power balance can be viewed in Figure 4.1. We can see that the system's power source is PV and DG. PV presents high power during the day and can generate much electricity, but at night the power is 0. The main power consumption of the system is electrical loads and hydrogen devices.

4.3 H2 balance

Figure 4.2 shows H2 balance in the six scenarios. We keep generating H2 all the time and most of the H2 are used for P2G equipment to generate gas. In addition, we can see that H2 out and H2 in would be appear in the same time, which indicates that the decision binary variables we relax in the implement is available.

4.4 CO2 balance

The Figure 4.3 indicates the CO2 balance in the six scenarios. CCS equipment keep generating CO2 and electricity. The CO2 generated are used for P2G system to generate gas. In addition, most of the CO2 are used to produce gas, while few of them are stored in our system.

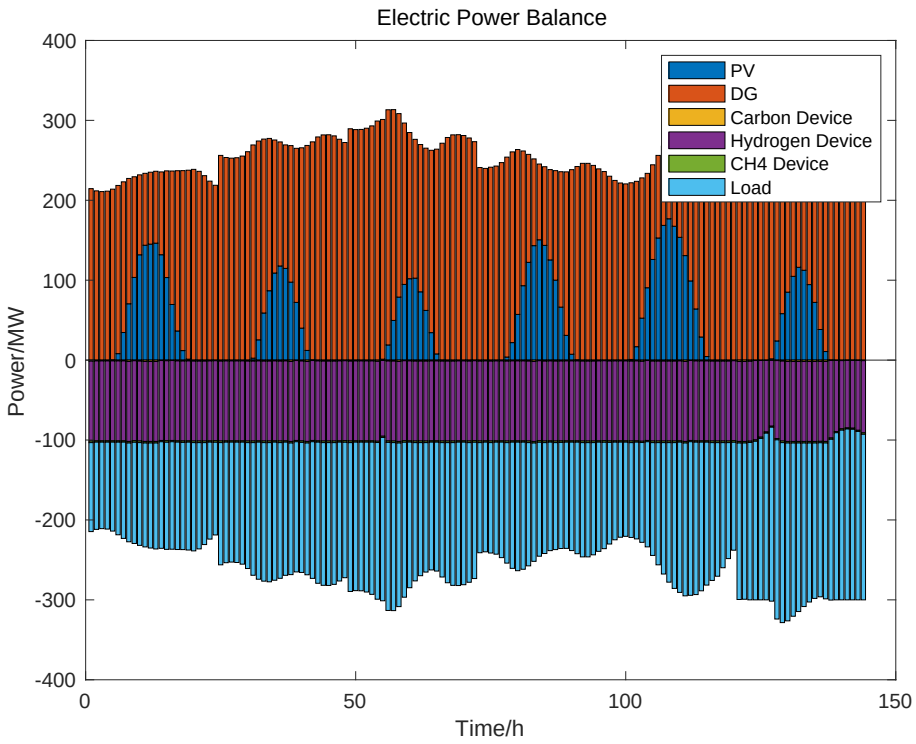

Figure 4.1: Electric power balance

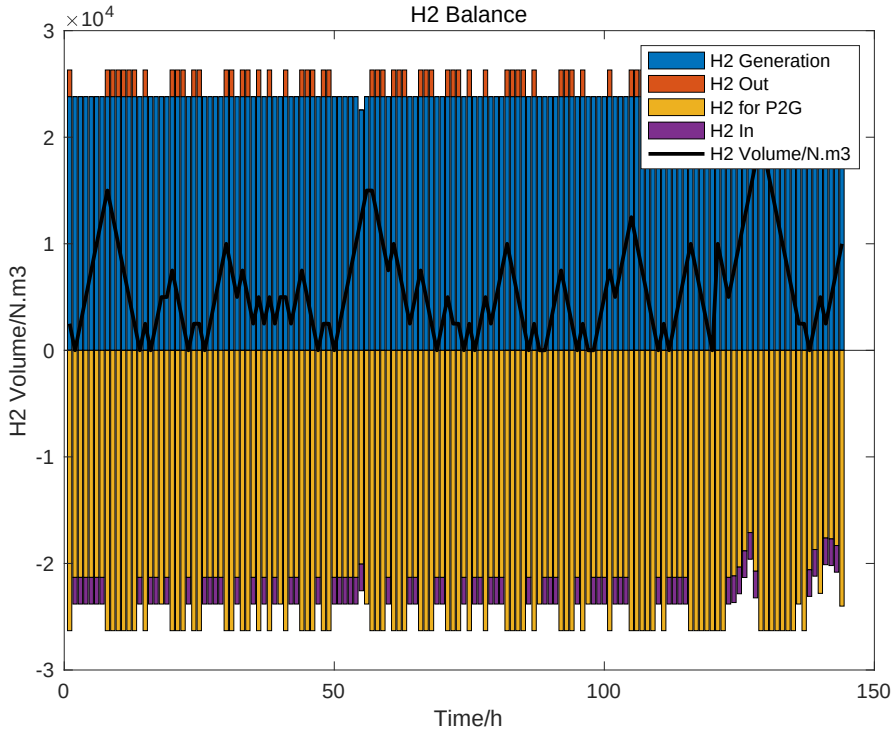

Figure 4.2: H2 balance

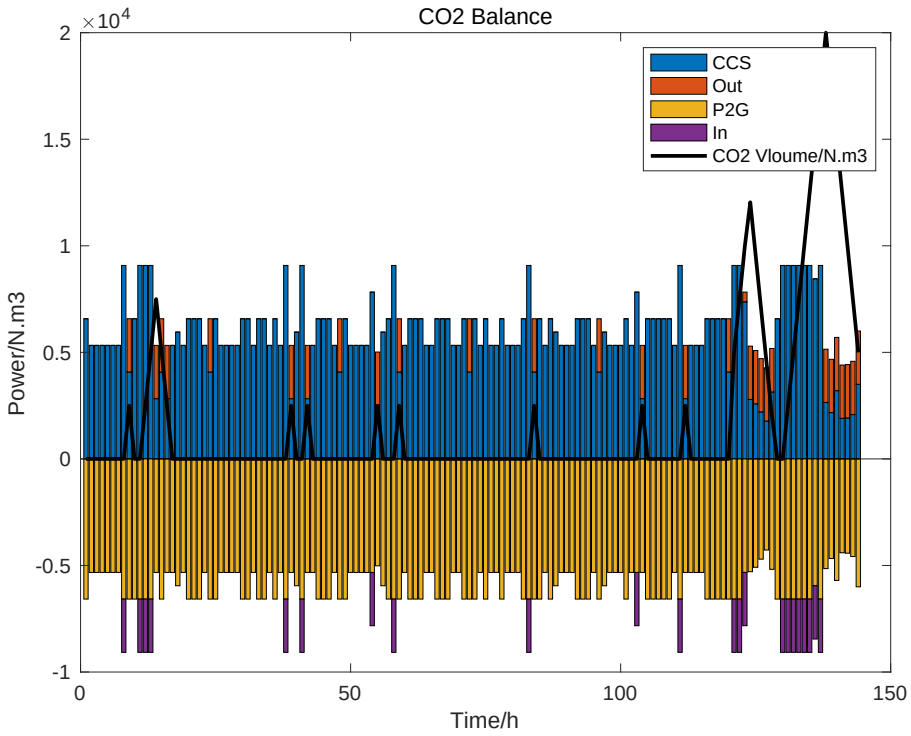

Figure 4.3: CO2 balance

5 Conclusion

In this paper, we develop a two-stage stochastic programming model for the microgrid planning and operation problem and apply multi-cut L-shape algorithm to solve it. In the first stage, optimal capacities of DG, RESs, hydrogen devices, and carbon devices are attained. In the second stage, optimal operation of the microgrid is obtained. Especially, integer variables representing hydrogen and gas production are relaxed and integrated into the two-stage stochastic programming. Uncertainties including RESs power output and load demand are involved.

References

[1] X. Cao, X. Sun, Z. Xu, B. Zeng, and X. Guan, "Hydrogen-based networked microgrids planning through two-stage stochastic programming with mixed-integer conic recourse," *IEEE Transactions on Automation Science and Engineering*, vol. 19, no. 4, pp. 3672–3685, 2021.

[2] L. Zhang, J. Kuang, B. Sun, F. Li, and C. Zhang, "A two-stage operation optimization method of integrated energy systems with demand response and energy storage," *Energy*, vol. 208, p. 118423, 2020.

[3] X. Zhou, Q. Zhao, Y. Zhang, and L. Sun, "Integrated energy production unit: An innovative concept and design for energy transition toward low-carbon development," *CSEE Journal of Power and Energy Systems*, vol. 7, no. 6, pp. 1133–1139, 2021.

[4] Y. Li, F. Zhang, Y. Li, and Y. Wang, "An improved two-stage robust optimization model for cchp-p2g microgrid system considering multi-energy operation under wind power outputs uncertainties," *Energy*, vol. 223, p. 120048, 2021.

[5] X. Shen, Q. Guo, and H. Sun, "Regional integrated energy system planning considering energy price uncertainties: a two-stage stochastic programming approach," *Energy Procedia*, vol. 158, pp. 6564–6569, 2019.

[6] M. Mazidi, A. Zakariazadeh, S. Jadid, and P. Siano, "Integrated scheduling of renewable generation and demand response programs in a microgrid," *Energy Conversion and Management*, vol. 86, pp. 1118–1127, 2014.

[7] S. Pazouki, M.-R. Haghifam, and A. Moser, "Uncertainty modeling in optimal operation of energy hub in presence of wind, storage and demand response," *International Journal of Electrical Power & Energy Systems*, vol. 61, pp. 335–345, 2014.

[8] R. M. Van Slyke and R. Wets, "L-shaped linear programs with applications to optimal control and stochastic programming," *SIAM journal on applied mathematics*, vol. 17, no. 4, pp. 638–663, 1969.

[9] J. R. Birge and F. V. Louveaux, "A multicut algorithm for two-stage stochastic linear programs," *European Journal of Operational Research*, vol. 34, no. 3, pp. 384–392, 1988.